Journal of Colloid and Interface Science 346 (2010) 163–171

Contents lists available at ScienceDirect

Journal of Colloid and Interface Science

www.elsevier.com/locate/jcis

Turbidity diagrams of polyanion/polycation complexes in solution as a potential tool to predict the occurrence of polyelectrolyte multilayer deposition

Hajare Mjahed [a,b], Jean-Claude Voegel [a,b], Armelle Chassepot [a,b], Bernard Senger [a,b], Pierre Schaaf [c], Fouzia Boulmedais [c], Vincent Ball [a,b,*]

[a] Institut National de la Santé et de la Recherche Médicale, Unité Mixte de Recherche 977, 11 rue Humann, 67085 Strasbourg Cedex, France
[b] Université de Strasbourg, Faculté de Chirurgie Dentaire, 1 Place de l'Hôpital, 67000 Strasbourg, France
[c] Centre National de la Recherche Scientifique, Institut Charles Sadron, Unité Propre 22, 23 rue du Loess, BP 84047, 67034 Strasbourg Cedex 2, France

ARTICLE INFO

Article history:
Received 21 January 2010
Accepted 18 February 2010
Available online 21 February 2010

Keywords:
Polyelectrolyte multilayer films
Polyelectrolyte complexes

ABSTRACT

Surface functionalization with polyelectrolyte multilayer films (PEM films) has become very popular owing to its simplicity and versatility. However, even if some research is already available, this field of surface chemistry lacks a systematic knowledge of how the polyelectrolyte structure and solution conditions influence the growth of PEM films. In this investigation, we focus on the possible relationship between turbidity of polycation and polyanion mixtures in solution, and the buildup of PEM films made from the same polyelectrolytes in the same physicochemical conditions, namely pH, temperature and ionic strength. It comes out that for six different polycation/polyanion combinations there is a clear correlation between the turbidity evolution of polycation/polyanion complexes with the salt concentration and the evolution of the film deposition with the same parameter. In this investigation, the complexes in solution were prepared in conditions where the ratio between the number of cationic to anionic groups was close to unity. Even if there is a correlation between turbidity in solution and PEM film deposition, we found some exceptions in the low salt concentration regime.

This work is an extension of the preliminary works of Cohen Stuart (D. Kovačević et al. Langmuir 18 (2002) 5607–5612) and Sukishvili et al. (S.A. Sukhishvili, E. Kharlampieva and V. Izumrudov, Macromolecules 39 (2006) 8873–8881).

1. Introduction

The coating of surfaces, with functional molecules to yield films with controlled properties and thickness, is of major importance for both its fundamental aspects and its applications in technology. The first demonstration of the possibility to use electrostatic self-assembly (ESA) to deposit multilayer films from colloids [1] as well as the generalization of the concept to polyelectrolytes [2–6] and to polyelectrolytes in combination with charged colloids [7–11] (among them biomolecules like DNA [12], proteins [13–16] polysaccharides [17] and even cells [18]) has opened the route to the easy and versatile coating of substrates with films having a thickness ranging from a few nanometers up to several micrometers. The layer-by-layer (LBL) deposition can rely on ESA as well as on the self-assembly of molecules carrying complementary functionalities, for instance polymers carrying hydrogen donor or acceptor moieties [19–22]. Charge transfer [23,24] and host–guest interactions [25] can also be used to build films using the layer-by-layer concept. Multilayer films can be obtained from two multifunctional molecules A and B provided that the functionality of A overcompensates that of B during the alternate adsorption. In the case of polyelectrolytes, the driving force for the deposition of a polyelectrolyte multilayer (PEM) film is the charge overcompensation at the topmost part of the film at each deposition step, as has been demonstrated by means of zeta potential measurements [26–28]. The PEM films are easy to deposit on various substrates, among them colloids [29,30] where they offer a plethora of possible applications in biology [31,32] as well as in materials science [33–35]. In addition, they can be deposited by regular solution coating (using dipping machines), by spin coating [36,37] or by spray [38,39].

The ease of the processing of such films is in total contrast with the complexity of the underlying deposition mechanism. To understand PEM deposition at a molecular level, two major aspects have to be fully understood:

(i) The origin of the internal charge compensation, which can be either of intrinsic [40,41] or of extrinsic nature [5,42,43], meaning that electroneutrality in the bulk of the film is due to the quantitative ion pairing between the polycation and

* Corresponding author. Address: Institut National de la Santé et de la Recherche Médicale, Unité Mixte de Recherche 977, 11 rue Humann, 67085 Strasbourg Cedex, France. Fax: +33 3 68 85 33 79.
E-mail address: vincent.ball@medecine.u-strasbg.fr (V. Ball).

0021-9797/$ - see front matter © 2010 Elsevier Inc. All rights reserved.
doi:10.1016/j.jcis.2010.02.042

the polyanion or to the incorporation of an excess of small electrolytes, respectively.

(ii) The understanding of the film growth regime. Indeed, three different situations have been described in the case of polyelectrolytes:

Linear growth, in which the film thickness as well as the amount of deposited molecules increase linearly with the number of deposited layer pairs, n. A layer pair results from the successive deposition of a polycation and a polyanion or vice versa. This film growth regime is by far the most common, the combination of poly(sodium-4-styrene sulfonate) (PSS) and poly(allylamine hydrochloride) (PAH) at ambient temperature being one of the most representative examples [4,25,44].

Supralinear growth in which the second derivative of the film thickness with respect to n is positive. The first example of such growth has been found in the combination between poly(L-lysine) and sodium alginate [45] and many examples followed in the literature [46–51]. It has been demonstrated that the supralinear growth can be described by an exponential function in many cases. This growth regime is due to diffusion of at least one of the participating polyelectrolytes in and out of the whole film during each deposition step [47]. This growth has been described by means of a model relying on the assumption that the deposition of one polyelectrolyte stops when its chemical potential in the bulk of the film is equal to its chemical potential in solution. In addition the last deposited layer constitutes an electrostatic potential barrier impeding the release of the polyelectrolytes from the film in the solution before the contact with the solution containing the polyelectrolyte of opposite charge [52]. Other models able to explain exponential growth of the film thickness have been proposed recently [53].

The absence of film growth which most often manifests in the adsorption of one polyelectrolyte followed by its near quantitative desorption when the substrate is put in contact with the polyelectrolyte of opposite sign [54,55]. This observation means that polyelectrolytes A and B prefer to form complexes that desorb from the substrate and are soluble in solution rather than to stick as an insoluble film on the substrate. These findings have been rationalized by Sukhishvili et al. in terms of phase diagrams [56].

In their model, which is an extension of that proposed by Cohen Stuart et al. [54], the formation of soluble complexes in solution is unfavorable to the deposition of PEMs. In contrast, the formation of insoluble complexes corresponds to a glassy state and the formation of PEM films when the same polyelectrolytes are deposited in LBL manner. This relationship between a turbidity diagram and multilayer buildup has been established on poly(methacrylic acid) and quaternized poly(vinyl pyridine) (QPVP) [56]. It has been demonstrated that the stability of polyelectrolyte–polyelectrolyte or polyelectrolyte-protein complexes (where the proteins have to be considered as colloids carrying a heterogeneous surface charge distribution) depends among other parameters on the chain length [57], the linear charge density of the polyelectrolyte [58–61], the ionic strength of the solution [62], the pH in the case of weak polyelectrolytes or proteins [62] and the temperature. Hence, the physicochemical parameters governing the interpolyelectrolyte complexation in solution appear to be basically the same as those governing the buildup of PEM films. For instance an increase in ionic strength of a solution containing already formed complexes or of a solution in contact with a PEM film leads finally to the solubilization of the complexes [63] (or a disappearance of the coacervate phase, where a coacervate corresponds to a liquid phase of insoluble complexes [64]) and the partial [65] or total dissolution of PEM films [66].

Exchange mechanisms provide another analogy between polyelectrolyte complexes and PEM films. One kind of polyelectrolyte in a polycation–polyanion complex can be displaced from these complexes by the introduction of a competing polyelectrolyte [67] and similarly exchange phenomena can occur in PEM films [68–70]. Finally, self assembled systems, polyelectrolyte complexes and PEM films can display variable mobility of their constituents: BSA diffuses as well in polyelectrolyte complexes [71] as in PEM films [72].

Despite these strong analogies in the behavior and properties of polyelectrolyte complexes and PEM films, there have been only few experimental investigations to uncover their molecular origin. Some isothermal titration microcalorimetry experiments suggest that the regime of film growth is related to the sign of the enthalpy during the complexation process in solution [73]. These data strongly suggest that entropy changes are one of the driving forces in both PE complexation [74] and PEM film buildup. The importance of entropic contributions to free energy changes during polyelectrolyte complexation has been assumed very early in the literature [75]. However, these entropy changes are difficult to measure by the sole use of isothermal titration calorimetry (ITC) [76,77].

All these investigations and analogies mentioned above between complexation in solution and growth of PEM films provide strong support to the assumption of Cohen Stuart et al. [54] and Sukishvili et al. [56].

In the present investigation, we aim to use a *broad range* of polyelectrolytes already involved in the preparation of PEM films, to attempt a correlation between the turbidity diagram of polycation–polyanion complexation behavior in solution and the possible buildup of PEM films from the same polyelectrolytes and to extend the qualitative rule introduced by Sukhishvili et al. [56] to the correlation between the turbidity diagram and the type of multilayer growth. Note that we use the denomination of "turbidity diagram" rather than the concept of phase diagram because the latter one requires the system to be at equilibrium. It is well known that PE complexes and films can correspond to kinetically frozen states [54]. Hence, the measurement of turbidity in solution at a given time after mixing the polyanion and polycation is a snapshot of the complexation process that may not correspond to the state of lowest free energy. If the polycation–polyanion association in solution, which will be measured by means of turbidity, is related to the growth of PEM films, it will provide a very easy, predictive tool for the to buildup of PEM films. The prediction merely would require to mix polycation and polyanion solutions in different solution conditions (pH, ionic strength) and to follow if phase separation occurs.

Our investigation will also highlight, as already suggested by Sukishvili et al. [56], that polymers carrying sulfonate groups are very efficient to produce stable polyelectrolyte complexes as well as robust buildup of PEM films over a broad range of physicochemical conditions. To be as general as possible, we used both polycarboxylates (poly(sodium-L-glutamate), PGA, sodium hyaluronate, HA, and polysulfonates (poly(sodium-4-styrene sulfonate), PSS. The used polycations carried both primary amine groups (poly(allylamine hydrochloride), PAH, and poly(L-lysine), PLL) and quaternary ammonium groups (poly(diallyldimethylammonium chloride), PDADMAC). Our investigation will also point out that there can be some exceptions in the relationship between the occurrence of turbidity and the (apparent) absence of film growth at low ionic strength.

2. Materials and methods

2.1. Polyelectrolyte solutions

Poly(L-lysine) (PLL, ref: P2636, $M_w = 2.92 \times 10^4$ g/mol, $M_w/M_n = 1.64$), poly(L-lysine) labeled with fluorescein isothiocyanate

(PLL^{FITC}, $M_w = 5.89 \times 10^4$ g/mol, $M_w/M_n = 2.82$) with an average of 0.008 FITC group per lysine monomer, poly(diallydimethylammonium chloride) (PDADMAC, $M_w = 9.36 \times 10^5$ g/mol), poly(allylamine hydrochloride) (PAH, $M_w = 7 \times 10^4$ g/mol), poly(sodium-4-styrene sulfonate) (PSS, $M_w = 7.0 \times 10^4$ g/mol), poly (sodium-L-glutamate) (PGA, $M_w = 4.75 \times 10^4$ g/mol), poly(ethylene imine) (PEI, $M_w = 75 \times 10^4$ g/mol, were purchased from Sigma (St. Quentin Fallavier, France). Sodium hyaluronate (HA, ref: 80190, $M_w = 3.81 \times 10^5$ g/mol, $M_w/M_n = 1.76$) was purchased from Lifecore (Chaska, MN). The mass distributions of HA and PLL were determined by means of steric exclusion chromatography–multi angle laser light scattering (SEC-MALLS).

NaCl aqueous solutions were prepared at different ionic strengths, and buffered at pH 7.4 with 1 mM Hepes (4-(2-hydroxyethyl)-1-piperazineethanesulfonic acid) for PLL and HA solutions or with 10 mM tris (tris(hydroxymethyl)aminomethane) to dissolve all other polyelectrolytes, using ultrapure water (MilliQ-plus system, Millipore) with a resistivity of 18.2 MΩ cm. The ionic strength of all the solutions was adjusted by adding variable amounts of NaCl.

Polyelectrolyte solutions were prepared by dissolution of adequate amounts of polyelectrolyte powders (or by dilution of the commercial solution in the case of PDADMAC) in 1 mM Hepes or 10 mM tris–NaCl buffer at pH 7.4. The solutions were freshly prepared before every buildup or turbidity measurement and equilibrated overnight in a closed vessel. HA and PLL solutions were prepared at a concentration of 3×10^{-3} M in monomer units. All other polyelectrolyte solutions were prepared at a concentration of 1 mg/mL, hence typically at a monomer concentration between 5×10^{-3} and 1×10^{-2} M in monomer units.

2.2. Buildup of polyelectrolyte multilayers

The PLL/HA and PDADMAC/PSS films, aimed to be imaged by means of confocal laser scanning microscopy (CLSM), were deposited with a dipping robot (Riegler & Kirstein GmbH, Potsdam, Germany) on glass slides (glass coverslips from Menzel GmbH & Co, Braunschweig, Germany). Before polyelectrolyte adsorption, the glass slides were cleaned with 0.1 M sodium dodecyl sulfate (15 min), 0.1 M HCl (15 min), and pure water. Then, the glass slides were dipped in a polycation solution for 8 min. A rinsing step was performed by dipping the substrates for 10 min in the NaCl containing buffer (pH 7.4). The polyanion was then deposited in the same manner. The buildup process was pursued by alternated depositions of the polycation and the polyanion. The film obtained after deposition of n layer pairs is denoted $(\text{polycation/polyanion})_n$. All the buildup experiments were performed at (25 ± 2)°C.

2.3. Confocal laser scanning microscopy (CLSM)

Confocal laser scanning microscopy investigations were performed on films in contact with a NaCl solution. These observations were carried out with a Zeiss LSM-510 microscope using a 40×/1.4 oil immersion objective and a 0.43-μm z-section interval. For all CLSM observations unless otherwise stated, the adsorption of PLL^{FITC} (respectively PSS^{Rho}) was performed by dipping the multilayer films for 15 min in a PLL^{FITC} (respectively PSS^{Rho}) solution and rinsing with 1 mM Hepes or 10 mM-tris buffer at pH 7.4 before its observation. FITC fluorescence was detected upon excitation at 488 nm, through a cut-off dichroic mirror and an emission band-pass filter of 505–530 nm (green). Rhodamine fluorescence was detected upon excitation at 543 nm and an emission long-pass filter above 585 nm (red emission). Virtual vertical sections can be visualized, allowing the film thickness to be determined. PSS was labeled with rhodamine according to the literature [78].

2.4. Quartz cristal microbalance with dissipation monitoring (QCM-D)

The construction of PEM films was monitored *in situ* by quartz crystal microbalance with dissipation monitoring QCM-D-E4 (Q-Sense, Götenborg, Sweden). The device was fitted with a 4-sensor chamber meaning that 4 buildup experiments could be performed simultaneously. The QCM-D technique consists in measuring the resonance frequency changes (Δf) of a quartz crystal induced by polyelectrolyte adsorption on this crystal, when compared to the same crystal in contact with the buffer solution. The quartz crystal is excited at its fundamental frequency (about 5 MHz), and the measurements are performed at the first, third, fifth and seventh overtones (denoted by $v = 1, 3, 5$ and 7, respectively) corresponding to about 5, 15, 25, and 35 MHz, respectively. Changes in the resonance frequencies, Δf_v, and in the relaxation time of the vibration once the excitation is switched off are measured at these four frequencies. The relaxation time gives access to the dissipation factor, D. The used quartz crystal is coated with a ~50 nm SiO_2 film. The four sensors are fixed in removable flow modules with inlet and outlet tubings through which the polyelectrolyte and buffer solutions are injected. In each experiment, 600 μL of NaCl solution was injected into the measurement cell. After stabilization of the signals (shift in reduced frequency, $\Delta f_v/v$, typically lower than 0.5 Hz/min), 600 μL of the polycation solution dissolved in a NaCl containing buffer was injected. This solution was left in the cell for 5 min, rinsed with the NaCl containing buffer solution and left again for 5 min. During the whole process, the frequency shifts were continuously recorded as a function of time. The same procedure was used for the deposition of the polyanion. The construction was pursued by alternate depositions of polycation and polyanion. A positive shift in the opposite of the reduced frequency shift, $-\Delta f_v/v$, can be associated, in first approximation, with an increase of the mass adsorbed on the crystal [79]. For all the investigated polycation–polyanion combinations, the adsorption kinetics reached a steady state in less than 5 min, the reduced frequency shift being smaller than 0.5 Hz/min.

2.5. Ellipsometry

Some of the PEM films were characterized by means of ellipsometry in the dry state (Horiba Jobin Yvon model PZ2000, Longjumeau, France). The measurements were performed at constant angle of incidence (70°) and at constant wavelength (632.8 nm) to determine the thickness of the silicon oxide atop the silicon chip as well as the thickness of the polyelectrolyte adlayer. The refractive index of the silicon oxide as well as that of the PEM film was fixed at 1.465 for all polyelectrolyte combinations. The thickness of the silicon oxide layer was subtracted from the whole deposit thickness to yield the thickness of the PEM film. Ellipsometry was used in a qualitative way to confirm the PEM thickness evolution with the ionic strength.

2.6. Turbidity as a function of mixing ratio (r) of polyelectrolytes and as a function of ionic strength

Mixtures of different couples of polycation/polyanion were prepared at different mixing ratios and at different ionic strengths in NaCl (the buffer always containing 1 mM Hepes or 10 mM tris at pH 7.4 depending on the polyelectrolyte combination). During the complex preparation, a given volume of the polycation solution was injected in a given volume of buffer containing the polyanion. The mixture was vigorously stirred to ensure fast homogenization. It has to be noted that we decided, purposely, to mix the polycation and polyanion in this order. Nevertheless, we performed some control experiments in which the polyanion solution was injected in the polycation solution. For some polycation–polyanion

combinations (PAH/PSS for instance) the turbidity values were dependent on the mixing order, but in all cases the turbidity change as a function of the ionic strength followed the same qualitative evolution. Hence, we will focus on experiments in which the polycation solution was injected in the polyanion solution. This way of preparing polycation–polyanion mixtures may not lead to equilibrium configurations but it mimics the procedure used to prepare the PEM films in which a polyelectrolyte solution is put in contact with a film already ending with an oppositely charged polyelectrolyte. To prepare polyelectrolyte complexes at equilibrium, it may be better to mix them in non-interacting conditions, for instance at very high ionic strength and to subsequently dialysis them against the desired buffer in order to produce conditions favorable for polyelectrolyte–polyelectrolyte interactions. This method of complex preparation is extremely time consuming and does not mimic the preparation of PEM films, therefore we did not use it.

In a typical experiment, performed at (25 ± 2)°C, a given volume of an aliquot of the polycation solution was added to an aliquot of the polyanion solution to establish different molar ratios between polycation and polyanion at different ionic strength of NaCl buffered solution in a polystyrene cuvette. The total volume of the polycation–polyanion mixture was always of 1 mL. A different cuvette was used for each value of the mixing ratio r which was varied between 0 (no polycation) and 10 corresponding to a large excess of polycation monomers. r is defined as the ratio between the number of moles of cationic units and the number of moles of anionic units. In the case of PSS (respectively PDADMAC) each monomer carries one elementary negative (respectively positive) charge. We make the assumption that a weak polyelectrolyte is highly protonated (case of the polyamines) or highly deprotonated (case of the polyacids). This assumption is realistic at pH 7.4 which is well below the average pKa of the polyamines (around 10 for PLL and 8.8–9 for PAH [80]) and far above the pKa of the used polyacids (4.5 for PGA). The validity of this assumption is also better at higher ionic strength where the intramolecular electrostatic repulsions between like charges are screened.

In order to have absorbance values lower than 2 (corresponding to the appearance of nonlinear absorbance–concentration relationship), 3 mL of buffer solution were added immediately to the polyanion–polycation mixture (1 mL of total volume), unless otherwise stated. The obtained solution was then aged for 10 min at room temperature before absorbance measurement.

The occurrence of complexation was quantified as the apparent absorbance at 500 nm, which corresponds to light scattering because none of the used polyelectrolytes absorbs light at this wavelength. This phenomenon is called turbidity. Spectrophotometric measurements were performed using a UV mc^2 spectrophotometer (Safas, Monaco).

3. Results and discussion

We will first investigate two polycation–polyanion combinations that are known to display different behaviors at 25 °C, an ionic strength of 0.15 M and at pH 7.4: the thickness of $(PLL/HA)_n$ films grows exponentially [46,47], whereas the $(PAH/PSS)_n$ films display a linear growth regime [44]. However, it has to be noted that the PAH/PSS combination can also lead to a supralinear growth regime at temperatures higher than 55 °C [81] or at high (>1 M) ionic strength [82]. Fig. 1 shows the turbidity diagram for the PLL/HA combination where the absorbance at 500 nm of the mixture is plotted as a function of r at different ionic strengths of NaCl. The reported absorbances were measured 10 min after mixture of the polycation and polyanion solutions. After longer times we observed either sedimentation or a progressive decrease in absorbance depending on the polycation/polyanion combination as well as on the ionic strength. Typically, the reduction in absorbance, due either to sedimentation (hence macroscopic phase separation) or to another process, was the most pronounced at $r \approx 1$, i.e. at charge equivalence between the polycation and the polyanion. This phenomenon is well known in the literature [83]. Because of the absence of a steady state in turbidity as a function of time for polycation/polyanion mixtures satisfying to $r \approx 1$, the notion of turbidity diagram is used in a qualitative manner only.

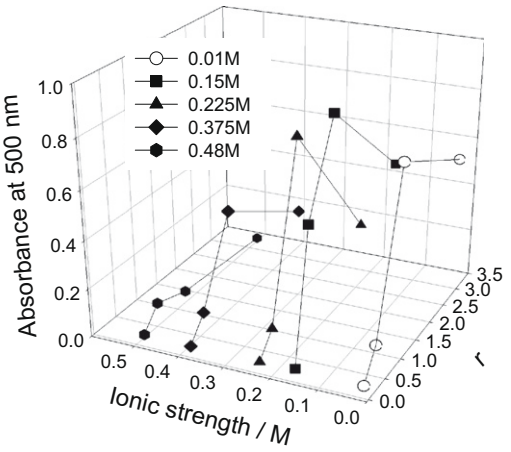

Fig. 1. Turbidity diagram, representing the turbidity (quantified as the absorbance at 500 nm) of the PLL/HA combination of polyelectrolytes as a function of the mixing ratio r and the ionic strength (adjusted with NaCl). The ionic strength values are indicated in the inset.

It is not the aim of this work to investigate whether the PE complexes sediment or undergo another evolution with time. This will be the subject of a forthcoming work. In the particular case of the PLL/HA combination the turbidity of the solution at $r \approx 1$ decreased progressively as a function of time without apparent sedimentation (Fig. 1 of the Supporting information). In the recent literature, it appears that PE complexes made from polyelectrolyte–neutral block copolymers can rearrange slowly, with characteristic times of hours [84]. We hypothesize that the PLL/HA complexes also follow this trend.

In opposition to the PLL/HA system, the PAH/PSS complexes display a clear sedimentation at mixing ratios close to 1 after only a few minutes in the ionic strength range between 0.1 and 5 M in NaCl. Whatever the final evolution of the polyelectrolyte complexes (phase separation or slow decrease in turbidity), for all the "turbidity diagrams" investigated in this work, the maximal turbidity is obtained close to $r = 1$ at all ionic strengths. This means that in this region either the number of PE complexes is maximal or their size is maximal, or a combination of both effects. We did not focus on the size distribution of the complexes: they are polydisperse and there are aggregates in the solution that can be bigger than a few μm particularly for the PAH/PSS and PAH/PGA combinations. Therefore, we will focus on the turbidity at $r \approx 1$ as a function of the ionic strength for all the investigated polycation/polyanion combinations. The turbidity for the PLL/HA and PAH/PSS combinations are plotted in Fig. 2 as a function of the ionic strength at $r \approx 1$. Note that a mixing ratio of 1 is representative for PEM films whose electroneutrality is ensured by means of intrinsic compensation, i.e. without need for small electrolyte incorporation. This is not necessarily the case, but anyway even in the case of extrinsic compensation, the ratio of the number of positive charges to the number of negative charges in the PEMs is never so far away from 1 [5]. Hence we assume that a mixing ratio of 1 in solution is representative, in a qualitative manner, of the polycation–polyanion mixture present in the PEM film.

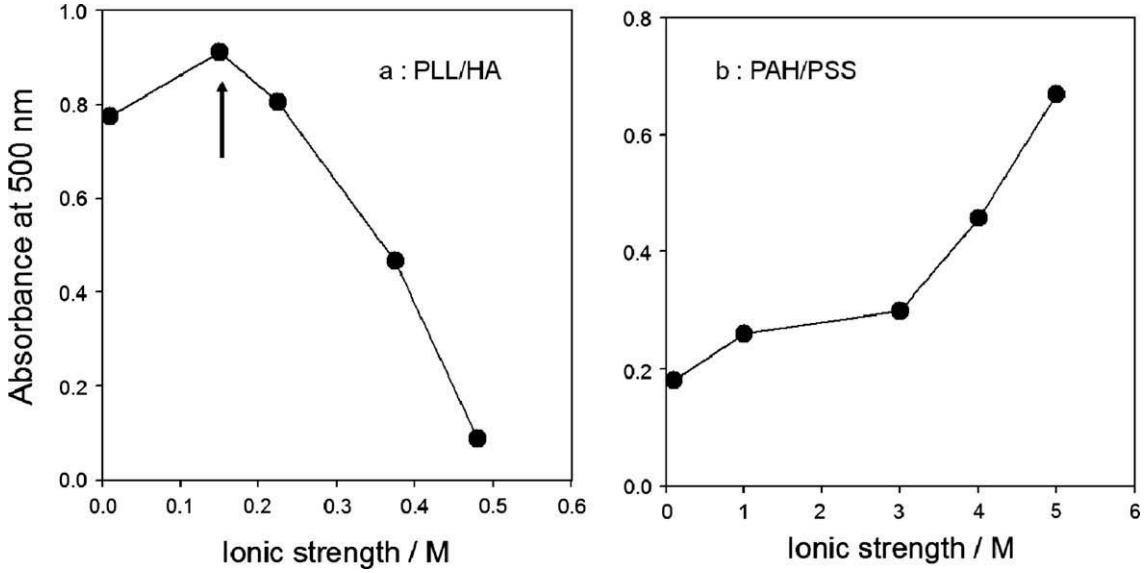

Fig. 2. Turbidity, quantified as the absorbance at 500 nm, of PLL/HA and PAH/PSS mixtures at $r \approx 1$ as a function of the ionic strength in NaCl. The arrow indicates the approximate position of the maximal turbidity in the case of the PLL/HA mixtures. The turbidity curve for the PLL/HA corresponds to the intersection of the diagram in Fig. 1 with the plane defined by $r = 1$ and parallel to the ionic strength and absorbance axes. The lines are aimed to guide the eye. Note that the two first points in part a were obtained at ionic strengths of 10 and 150 mM.

It appears that the two systems behave rather differently: the extent of PLL/HA complexation seems to reach a maximum at around 0.15 M in NaCl whereas at 0.48 M in NaCl, the solution is fully transparent. Examination of the PLL/HA mixture at $r \approx 1$ in these conditions of high ionic strength by means of dynamic light scattering reveals the absence of complexes: the average hydrodynamic radius is close to that of HA and PLL in their individual solutions (data not shown), namely a few nanometers. This means that PLL and HA are not interacting strongly enough to form complexes in these conditions owing to strong screening of the electrostatic forces.

On the other hand, the turbidity evolution for the PAH/PSS combination does not display a maximum as a function of the ionic strength between 0.1 and 5 M. This means that an increase in ionic strength is not able to "soften" the PAH/PSS complexes sufficiently to dissociate them. In the present case, the extent of PAH/PSS complexation, as estimated by turbidity, is strong up to 5 M in ionic strength.

Let us now turn to the buildup of the PEM films using the same combinations of polyelectrolytes. Fig. 3 shows that the thickness reached after the deposition of six layer pairs ($n = 6$) is maximal at around 0.15–0.30 M in NaCl for the PLL/HA combination, whereas the film thickness increases monotonously for the PAH/PSS combination up to 5 M in NaCl. The same trend, namely the occurrence of the maximal thickness at an intermediate ionic strength, is observed for much thicker $(PLL/HA)_n$ films ($n = 50$ instead of $n = 6$) as investigated by means of CLSM (Fig. 2 of the Supporting information). In the case of PAH/PSS films, a monotonous

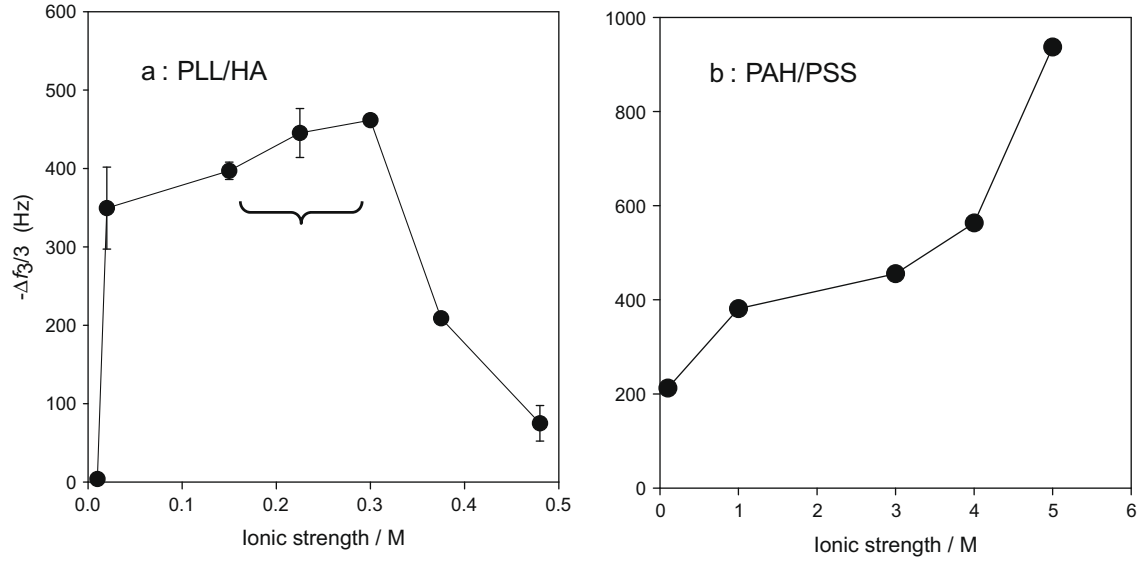

Fig. 3. QCM-D monitoring of PEM film deposition after six polycation/polyanion deposition steps in the case of the PLL/HA (a) and PAH/PSS (b) combinations. The lines are aimed to guide the eye and the error bars (when indicated) correspond to the standard deviation of three experiments. The curly bracket corresponds to the domain of ionic strength where the PLL/HA film buildup is maximal. Note that the two first points in part a were obtained at ionic strengths of 10 and 25 mM.

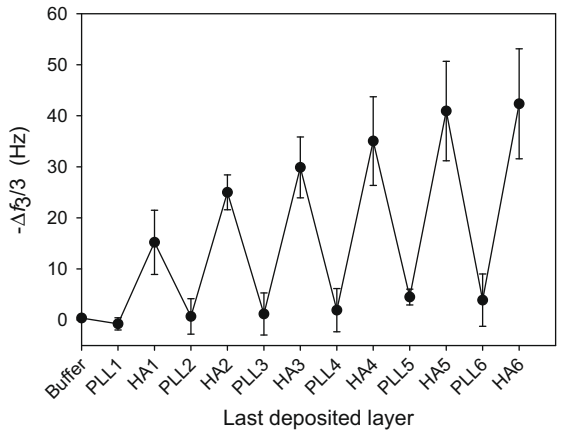

Fig. 4. Evolution of the reduced frequency (at the 3rd harmonic of the quartz crystal), monitored by QCM-D as a function of the nature of the adsorbing polyelectrolyte in the case of the PLL/HA combination in the presence of NaCl at 0.01 M. The error bars correspond to the standard deviation over two experiments and the lines are aimed to guide the eye.

increase in thickness is also found when the PEM films are characterized by ellipsometry in the dry state (Fig. 3 of the Supporting information).

Clearly the PEM film thickness (Fig. 3) follows *the trend* of the turbidity versus ionic strength (Fig. 2) with one exception: in the case of the PLL/HA combination, an important turbidity already appears at small ionic strength (10 mM) but almost no PEM deposition. Indeed, in this particular condition, the deposition of HA on a PLL covered substrate is followed by its nearly quantitative desorption upon contact with a PLL solution (Fig. 4). Note also that the position of the maximum in turbidity does not exactly match with the position of the mid of the broad maximum in the frequency change versus ionic strength in the case of the PLL/HA system. Hence the turbidity curve has to be used cautiously when aimed to predict the buildup behavior of the PEM film made from the same combination of polyelectrolytes.

Besides the region of low ionic strength, the trend for the PLL/HA and PAH/PSS combinations confirms the findings by Sukishvilli et al. [56], namely that the absence of high turbidity and hence of important PE complexation in solution seems to be related to the impossibility to buildup PEM films in the same physicochemical conditions.

We will now check if these findings can be generalized to other combinations of polycations and polyanions. Indeed there are already a few findings similar to the one we just reported for the PLL/HA and PAH/PSS combinations of polyelectrolyte [41,56], but to our knowledge there is no research report that investigates simultaneously several polycation/polyanion combinations.

Let us first consider the polycation/polyanion combinations in which the polyanion is a polycarboxylate. For the PLL/PGA as well as for the PAH/PGA system the turbidity versus NaCl concentration as well as the reduced frequency change monitored by QCM-D (hence in a first approximation, the amount of deposited film) versus NaCl concentration displays the same shape as for the PLL/HA system (Fig. 5).

More specifically, the NaCl concentration at which maximal turbidity is obtained at $r \approx 1$ matches closely the salt concentration at which the film thickness reaches a maximum value. In addition it

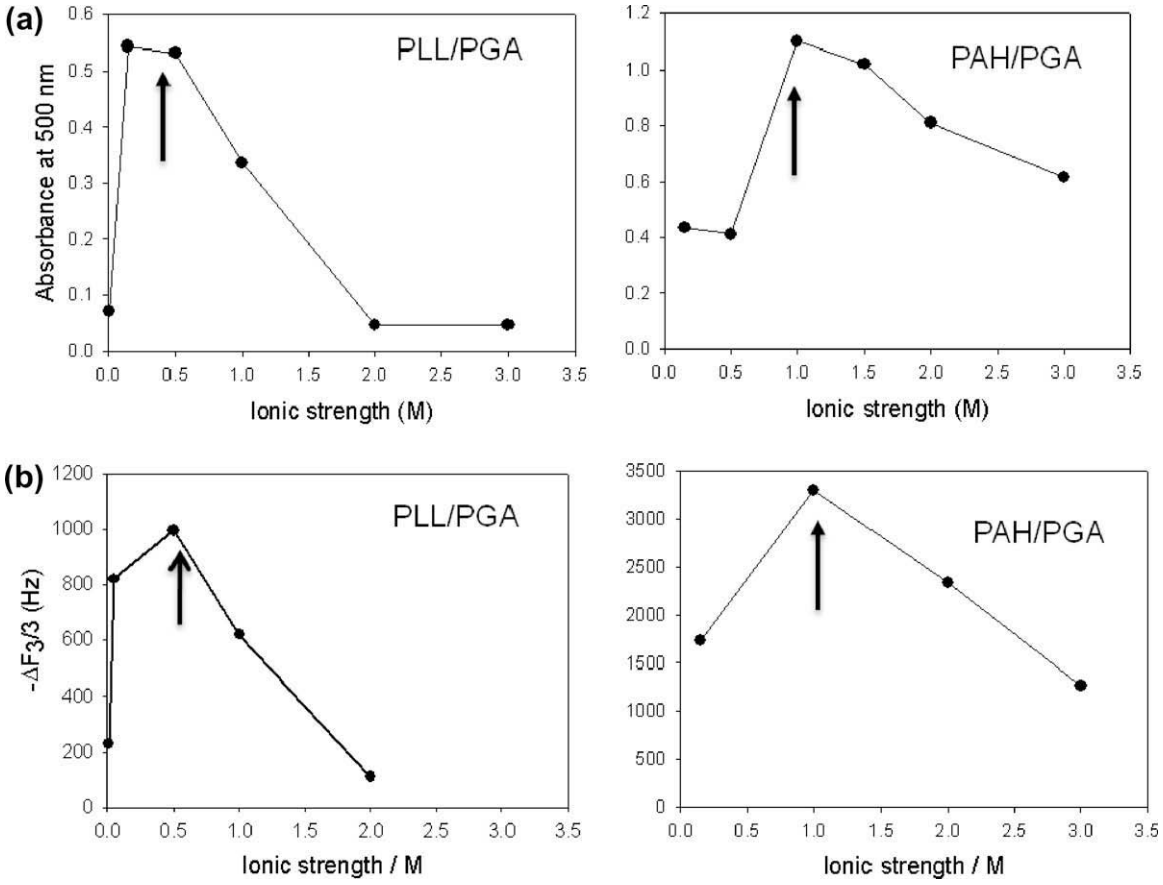

Fig. 5. Comparison between: (a) the turbidity (at 500 nm) versus ionic strength and (b) reduced frequency change versus ionic strength for the PLL/PGA and PAH/PGA systems. The reduced frequency changes (at $v = 3$) obtained by QCM-D are quoted in the case of six layer pairs. The arrows identify the positions of the maxima.

follows from Fig. 5 that the buildup of PEM films made from PGA as the polyanion is possible up to 3 M in NaCl in presence of PAH, whereas the film growth is not possible anymore above 2 M when PLL is used as the polycation. The trend found by QCM-D in the hydrated state is also confirmed for $(PLL/PGA)_{10}$ films whose thickness has been measured by ellipsometry in the dry state (Fig. 4 of the Supporting information). The difference in the maximal ionic strength at which $(PLL/PGA)_n$ and $(PAH/PGA)_n$ films can be deposited does presumably originate from structural differences between PLL and PAH. When compared to the PLL/HA combination, where the optimal ionic strength lies around 0.2–0.3 M, one observes that the buildup of the $(PLL/PGA)_n$ films is possible up to higher ionic strengths. This finding reflects the lower charge density of HA (one charged carboxylate every disaccharide) compared to that of PGA (one charged carboxylate every amino acid at pH 7.5 and in the presence of high ionic strength).

To go further in this direction, let us now consider the polyelectrolyte complexes as well as the PEM films made from the same polycations, namely PLL and PAH but the polyanion being PSS instead of PGA. The data for the PAH/PSS combination are given in Figs. 2 and 3: in the 0.01–5 M NaCl concentration range, both the solution turbidity (measured at $r \approx 1$) and the film thickness increase monotonously. Almost the same trend is found for the PLL/PSS combination, as shown in Fig. 6. In contrast with the PAH/PSS combination, however, the turbidity curve for the PLL/PSS combination displays a plateau extending up to 5 M in ionic strength and not a continuous increase.

This finding means for the two polycations, PLL and PAH, carrying primary ammonium groups, that the change in the polyanionic partner determines the complexation in solution and the buildup of the PEM films: in the presence of the carboxylate-carrying PGA, the complexation and film buildup display a maximum at intermediate ionic strengths, whereas no maximum appears up to 5 M in NaCl in the presence of the sulfonate-carrying PSS. Now consider the situation of a constant polyanion, PSS, put in the presence of either a polycation carrying primary amines (PLL and PAH) or quaternary ammonium groups (PDADMAC). It appears that when complexes are formed between PDADMAC and PSS, the turbidity versus NaCl concentration curve displays a marked maximum (at around 2 M) which corresponds closely to the ionic strength at which the PEM film thickness reaches its maximum (Fig. 7). The occurrence of a maximum in film thickness around 2 M in ionic strength was also found for $(PDADMAC\text{-}PSS^{Rho})_{30}$ films investigated by means of CLSM (Fig. 5 of the Supporting information).

Hence the change from PLL or PAH to PDADMAC deeply modifies the behavior of the PE complexes as well as that of the PEM film deposition: qualitatively the PDADMAC/PSS combination behaves as the PLL/HA (Figs. 2 and 3), as the PLL/PGA and as the PAH/PGA combinations (Fig. 5). Taken together these data confirm the trend extracted from the experiments performed by the group of Sukhishvili [56], namely that complexes made from polycations carrying primary amines and from polyanions carrying sulfate (not investigated herein) or sulfonate groups are particularly stable in a broad range of salt concentrations. Our investigation shows on the basis of six polycation/polyanion combinations, that it is possible to predict qualitatively the possibility to deposit multilayer films at a given pH and ionic strength by just mixing a polycation and a polyanion solution to reach a mixing ratio of 1: if the solution

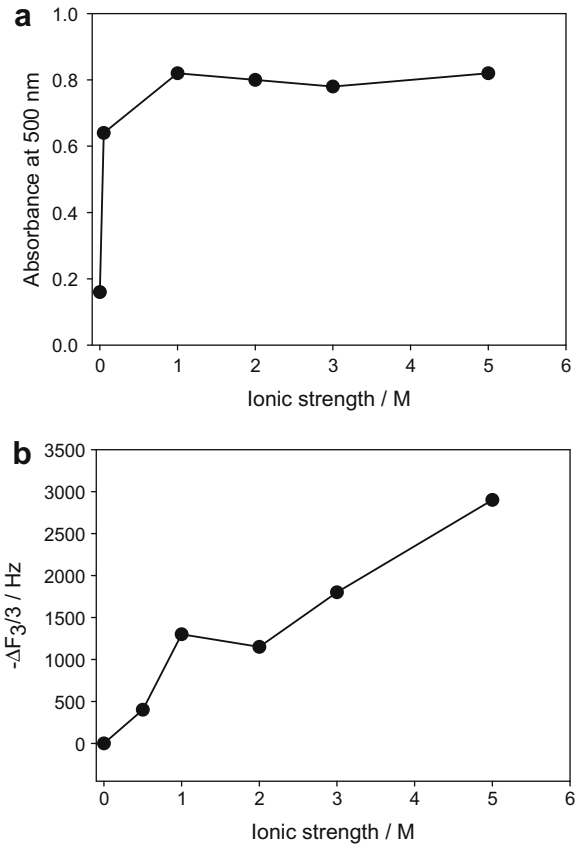

Fig. 6. Evolution of: (a) the turbidity for PLL/PSS mixtures at $r \approx 1$ as a function of the ionic strength and (b) evolution of the reduced frequency change (at $\nu = 3$) after the deposition of a $(PLL\text{–}PSS)_8$-PLL film as a function of the ionic strength. The lines are aimed to guide the eye.

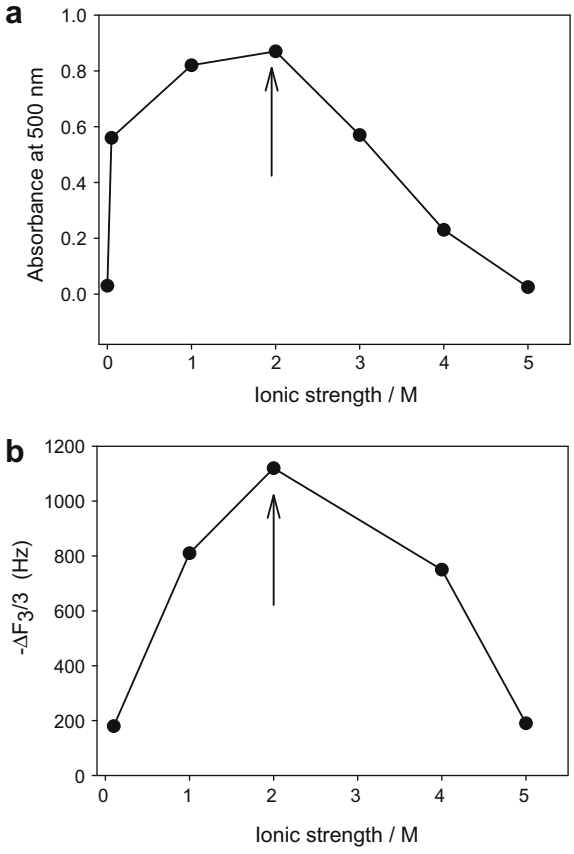

Fig. 7. Evolution of: (a) the turbidity for PDADMAC/PSS mixtures at $r \approx 1$ as a function of the ionic strength and (b) of the reduced frequency change (at $\nu = 3$) after the deposition of a $(PDADMAC\text{–}PSS)_{10}$ film as a function of the ionic strength. The lines are aimed to guide the eye and the arrows indicate the position of the maxima.

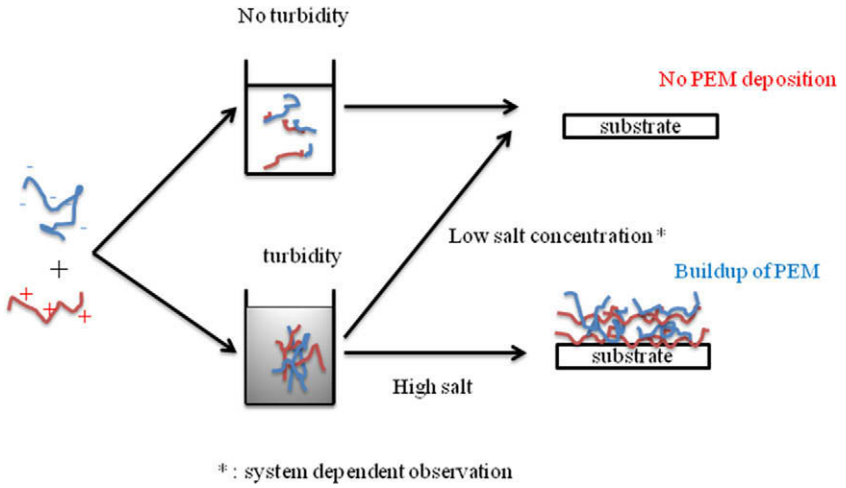

Scheme 1. Relationship between turbidity of polycation–polyanion mixtures (at $r \approx 1$) in solution and the buildup of PEM films.

turns immediately to turbid, it is a strong indication that the buildup of PEM films is possible under these conditions. When the solution remains transparent, particularly at high ionic strength, it means that the formation of soluble interpolyelectrolyte complexes and the absence of complexation are thermodynamically favored, which plays against the buildup of PEM films.

However, the analysis of turbidity in solution does not allow explaining all the behavior of PEM deposition. As seen from the PLL/HA (Fig. 2) as well as from the PAH/PGA (Fig. 5), PLL/PSS (Fig. 6) and PDADMAC/PSS (Fig. 7) combinations, the absence of film buildup or the slow film buildup at small ionic strength seems not related to the occurrence of PE complexation. The analysis of the film buildup for the PLL/HA combination at 0.01 M in NaCl provides an explanation: the film does not deposit because the introduction of the polycation in solution removes the polyanion that is already adsorbed, meaning that the formation of complexes is favorable but that they do not adhere strongly to the substrate (Fig. 4). Note however that the turbidity - film deposition correlation is perfect for the PAH/PSS combination (Figs. 2 and 3). Hence, taking all the investigated systems into account, the criterion of important turbidity in solution to predict the occurrence of film deposition is not necessarily valid at low ionic strength. However, at an ionic strength higher than a critical value, depending on the investigated system, there is a clear correlation between turbidity and PEM film buildup.

Based, on our findings with the six polycation–polyanion mixtures, we propose a general scheme to summarize our findings (scheme 1).

Such a qualitative scheme should help researcher in the field of PEM films to optimize the design of film architectures when using new polycation–polyanion combinations: in the absence of turbidity there should be no film deposition (this may originate from either too strong a screening at high ionic strength or from a too low a charge density of the polyelectrolytes [85]). But even if the solution displays high turbidity, the PEM film deposition may not occur owing to adsorption–desorption phenomena, particularly in the low ionic strength range.

4. Conclusions

In this report we have described additional evidence that there is a strong correlation between polyelectrolyte complexation in solution and PEM buildup in accordance with previous examples that have been provided in the literature [41,56]. Herein we rely on experiments performed on six polycation–polyanion combinations widely used in the investigation of PEM film properties, namely PLL/HA, PLL/PGA, PAH/PGA, PLL/PSS, PAH/PSS and PDADMAC/PSS. The different polycation/polyanion distinguish from one another by two markedly different behaviors: depending on the polyelectrolyte couple the turbidity versus NaCl concentration as well as the film deposition versus NaCl concentration have a maximum or not (with sometimes a plateau as for the PLL/PSS system). The combinations containing a polycarboxylic acid seem to give rise to curves displaying a maximum whereas the combinations containing the strong polyelectrolyte PSS show a monotonous behavior in turbidity as well as in film thickness with respect to the supporting salt (NaCl) concentration. The turbidity diagram of the PLL/PSS combination displays a plateau versus the ionic strength but not a defined maximum. However, when PSS is associated to a polycation containing quaternary ammonium groups, PDADMAC, the turbidity as well as film deposition versus NaCl concentration display again a defined maximum. These two kinds of behaviors are directly related to the interaction strength between the polycation and the polyanion. This interaction strength depends on the structure of the polyelectrolytes as well as on the physicochemical conditions in the solution (pH, ionic strength, temperature).

Anyway, the investigation of polyelectrolyte complexation in solution, particularly around charge equivalence ($r \approx 1$), is a powerful diagnostic tool to predict the fate of PEM deposition on surfaces. However, as exemplified for the PLL/HA and for the PDADMAC/PSS combinations, great care should be taken when trying to use turbidity diagrams at very low ionic strength where strong turbidity can be found whereas the film buildup is hindered by adsorption–desorption phenomena. Our qualitative tool to predict the occurrence of PEM deposition should hence be used only in the intermediate to high ionic strength domain. Clearly more research has to be devoted to the relationship between polyelectrolyte complexation in solution and deposition of PEM films on surfaces.

Acknowledgments

We thank Cosette Betscha for her help in the ellipsometry experiments. H.M. was supported by a fellowship from the "Ministère de la Recherche et de la Technologie".

Appendix A. Supplementary material

Supplementary data associated with this article can be found, in the online version, at Kinetics of the absorbance decrease at

500 nm for a PLL–HA mixture at $r = 1$, thickness of $(PLL–HA)_{50}$ films as a function of ionic strength as measured by CLSM, thickness of $(PAH\text{-}PSS)_{10}$ films as determined (in the dry state) by means of ellipsometry, thickness of $(PAH\text{-}PGA)_{10}$ films as determined (in the dry state) by means of ellipsometry and thickness of $(PDAD\text{-}MAC\text{-}PSS^{rho})_{30}$ multilayer films, measured by CLSM, as a function of the ionic strength. doi:10.1016/j.jcis.2010.02.042.

References

[1] R.K. Iler, J. Colloid Interface Sci. 21 (1966) 569–594.
[2] G. Decher, J.D. Hong, J. Schmitt, Thin Solid Films 210–211 (1992) 831-x.
[3] G. Decher, J. Schmitt, Prog. Colloid Polym. Sci. 89 (1992) 160–164.
[4] G. Decher, Science 277 (1997) 1232–1237.
[5] N.G. Hoogeveen, M.A. Cohen Stuart, G.J. Fleer, M.R. Böhmer, Langmuir 12 (1996) 3675–3681.
[6] D. Yoo, S.S. Shiratori, M.F. Rubner, Macromolecules 31 (1998) 4309–4318.
[7] S.W. Keller, H.-N. Kim, T.E. Mallouk, J. Am. Chem. Soc. 116 (1994) 8817–8818.
[8] N.A. Kotov, I. Dekany, J.H. Fendler, J. Phys. Chem. 99 (1995) 13065–13069.
[9] F. Caruso, H. Lichtenfeld, M. Giersig, H. Möhwald, J. Am. Chem. Soc. 120 (1998) 8523–8524.
[10] F. Caruso, D.G. Kurth, D. Volkmer, M.J. Koop, A. Müller, Langmuir 14 (1998) 3462–3465.
[11] M. Suda, Y. Einaga, Angew. Chem. Int. Ed. 48 (2009) 1754–1757.
[12] Y. Lvov, G. Decher, G.B. Sukhorukov, Macromolecules 26 (1993) 5396–5399.
[13] Y. Lvov, K. Ariga, I. Ichinose, T. Kunitake, J. Am. Chem. Soc. 117 (1995) 6117–6123.
[14] J.-I. Anzai, T. Hoshi, N. Nakamura, Langmuir 16 (2000) 6306–6311.
[15] L. Derbal, H. Lesot, J.-C. Voegel, V. Ball, Biomacromolecules 4 (2003) 1255–1263.
[16] R. Dronov, D.G. Kurth, H. Möhwald, F.W. Scheller, F. Lisdat, Angew. Chem. 47 (2008) 3000.
[17] L. Richert, Ph. Lavalle, E. Payan, X.Z. Shu, G.D. Prestwich, J.-F. Stoltz, P. Schaaf, J.-C. Voegel, C. Picart, Langmuir 20 (2004) 448–458.
[18] S. Krol, M. Nolte, A. Diaspro, D. Mazza, R. Magrassi, A. Gliozzi, A. Fery, Langmuir 21 (2005) 705–709.
[19] A.F. Xie, S. Granick, Macromolecules 35 (2002) 1805–1813.
[20] S.A. Sukhishvili, S. Granick, J. Am. Chem. Soc. 122 (2000) 9550–9551.
[21] S.A. Sukhishvili, S. Granick, Macromolecules 35 (2002) 301–310.
[22] J. Cho, F. Caruso, Macromolecules 36 (2003) 2845.
[23] Y. Shimazaki, R. Nakamura, S. Ito, M. Yamamoto, Langmuir 17 (2001) 953–956.
[24] T. Serizawa, K. Hamada, T. Kitamaya, N. Fujimoto, K. Hatada, M. Akashi, J. Am. Chem. Soc. 122 (2000) 1891–1899.
[25] A. Van der Heyden, M. Wilczewski, P. Labbé, R. Auzély, Chem. Commun. (2006) 3220–3222.
[26] G. Ladam, P. Schaad, J.-C. Voegel, J.C.P. Schaaf, G. Decher, F.J.G. Cuisinier, Langmuir 16 (2000) 1249–1255.
[27] F. Caruso, E. Donath, H. Möhwald, J. Phys. Chem. B. 102 (1998) 2011–2016.
[28] Z. Adamczyk, M. Zembala, M. Kolasinska, P. Warszynski, Colloids Surf. A (2007) 455–460.
[29] E. Donath, G.B. Sukhorukov, F. Caruso, S.A. Davis, H. Möhwald, Angew. Chem. Int. 37 (1998) 2202–2205.
[30] B.G. De Geest, N.N. Sanders, G.B. Sukhorukov, J. Demeester, S.C. De Smet, Chem. Soc. Rev. 36 (2007) 636–649.
[31] Y. Wang, A.S. Angelatos, F. Caruso, Chem. Mater. 20 (2008) 848–858.
[32] Z. Tang, Y. Wang, P. Podsiadlo, N.A. Kotov, Adv. Mater. 18 (2006) 3203–3224.
[33] K. Ariga, J.P. Hill, Q. Ji, PCCP 9 (2007) 2319–2340.
[34] J. Lutkenhaus, P.T. Hammond, Soft Matter 3 (2007) 804–816.
[35] M. Michel, A. Taylor, R. Sekol, P. Podsiadlo, P. Ho, N.A. Kotov, L. Thompson, Adv. Mater. 19 (2007) 3859–3864.
[36] P.A. Chiarelli, M.S. Johal, J.L. Casson, J.B. Roberts, J.M. Robinson, H.-L. Wang, Adv. Mater. 13 (2001) 1167–1169.
[37] C. Jiang, S. Markutsia, V.V. Tsukruk, Adv. Mater. 16 (2004) 157–161.
[38] J.B. Schlenoff, S.T. Dubas, T.R. Fahrat, Langmuir 16 (2000) 9968–9969.
[39] A. Izquierdo, S.S. Ono, J.-C. Voegel, P. Schaaf, G. Decher, Langmuir 21 (2005) 7558–7567.
[40] J.B. Schlenoff, H. Ly, M. Li, J. Am. Chem. Soc. 120 (1998) 7626–7634.
[41] J.B. Schlenoff, S.T. Dubas, Macromolecules 34 (2001) 592–598.
[42] E. Hübsch, G. Fleith, J. Fatisson, P. Labbé, J.-C. Voegel, P. Schaaf, V. Ball, Langmuir 21 (2005) 3664–3669.
[43] R. Takita, K. Yoshida, J.-I. Anzai, Sens. Actuators B 121 (2007) 54–60.
[44] J.J. Ramsden, Y.M. Lvov, G. Decher, Thin Solid Films 254 (1995) 246–251.
[45] D.L. Elbert, C.B. Herbert, J.A. Hubbell, Langmuir 15 (1999) 5355–5362.
[46] C. Picart, Ph. Lavalle, P. Hubert, J.F.G. Cuisinier, G. Decher, P. Schaaf, J.-C. Voegel, Langmuir 17 (2001) 7414–7424.
[47] C. Picart, J. Mutterer, L. Richert, Y. Luo, G.D. Prestwich, P. Schaaf, J.-C. Voegel, Ph. Lavalle, Proc. Natl. Acad. Sci. U. S. A 99 (2002) 12531–12535.
[48] Ph. Lavalle, C. Gergely, F.J.G. Cuisinier, G. Decher, P. Schaaf, J.-C. Voegel, C. Picart, Macromolecules 35 (2002) 4458–4465.
[49] F. Boulmedais, V. Ball, P. Schwinte, B. Frisch, P. Schaaf, J.C. Voegel, Langmuir 19 (2003) 440–445.
[50] E. Poptoshev, B. Schoeler, F. Caruso, Langmuir 20 (2004) 829–834.
[51] J. Fu, J. Ji, L. Shen, A. Küller, A. Rosenhahn, J.C. Shen, M. Grunze, Langmuir 25 (2009) 672–675.
[52] Ph. Lavalle, C. Picart, J. Mutterer, C. Gergely, H. Reiss, J.-C. Voegel, B. Senger, P. Schaaf, J. Phys. Chem. B 108 (2004) 635–648.
[53] N. Hoda, R.G. Larson, J. Phys. Chem. B 113 (2009) 4232–4241.
[54] D. Kovačević, S. Van der Burgh, A. de Keizer, M.A. Cohen Stuart, Langmuir 18 (2002) 5607–5612.
[55] D. Kovačević, S. Van der Burgh, A. de Keizer, M.A. Cohen Stuart, J. Phys. Chem. B 107 (2003) 7998–8002.
[56] S.A. Sukhishvili, E. Kharlampieva, V. Izumrudov, Macromolecules 39 (2007) 8873–8881.
[57] D. Takahashi, Y. Kubota, K. Kokai, T. Isumi, M. Hirata, E. Kokufuta, Langmuir 16 (2000) 3133–3140.
[58] H. Dautzenberg, W. Jaeger, Macromol. Phys. Chem. 203 (2002) 2095–2102.
[59] E.S. Trukhanova, V.A. Izumrudov, A.A. Litmanovich, A.N. Zelikin, Biomacromolecules 6 (2005) 3198–3201.
[60] K.W. Mattison, P.L. Dubin, I.J. Brittain, J. Phys. Chem. B 102 (1998) 3830–3836.
[61] E. Seyrek, P.L. Dubin, J. Henriksen, Biopolymers 86 (2007) 249–259.
[62] R.K. Hallberg, P.L. Dubin, J. Phys. Chem. B 102 (1998) 8629–8633.
[63] V.A. Izumrudov, M.V. Zhiryakova, Macromol. Chem. Phys. 200 (1999) 2533–2540.
[64] H.G. Bungenberg de Jong, H.R. Kruyt, Kolloidn. Zh. 50 (1930) 39.
[65] A.J. Nolte, N. Takane, E. Hindman, W. Gaynor, M.F. Rubner, R.E. Cohen, Macromolecules 40 (2007) 5479–5486.
[66] H. Mjahed, J.-C. Voegel, B. Senger, A. Chassepot, A. Rameau, V. Ball, P. Schaaf, F. Boulmedais, Soft Matter 5 (2009) 2269–2276.
[67] A. Zelikin, E.S. Trukhanova, D. Putnam, V.A. Izumrudov, A.A. Litmanovich, J. Am. Chem. Soc. 125 (2003) 13693–13699.
[68] V. Ball, E. Hübsch, R. Schweiss, J.C. Voegel, P. Schaaf, W. Knoll, Langmuir 21 (2005) 8526–8531.
[69] H.W. Jomaa, J.B. Schlenoff, Langmuir 21 (2005) 8081–8084.
[70] N.S. Zacharia, M. Modestino, P.T. Hammond, Macromolecules 40 (2007) 9523–9528.
[71] H.B. Bohidar, P.L. Dubin, P.R. Majhi, C. Tribet, W. Jaeger, Biomacromolecules 6 (2005) 1573–1585.
[72] L. Szyk, P. Schwinté, J.-C. Voegel, P. Schaaf, B. Tinland, J. Phys. Chem. B 106 (2002) 6049–6055.
[73] N. Laugel, C. Betscha, M. Winterhalter, J.-C. Voegel, P. Schaaf, V. Ball, J. Phys. Chem. B 110 (2006) 19443–19449.
[74] V. Ball, M. Winterhalter, P. Schwinté, Ph. Lavalle, J.-C. Voegel, P. Schaaf, J. Phys. Chem. B 106 (2002) 2357–2364.
[75] A.S. Michaels, Ind. Eng. Chem. 57 (1965) 32.
[76] C.B. Bucur, Z. Sui, J.B. Schlenoff, J. Am. Chem. Soc. 128 (2006) 13690–13691.
[77] X. Feng, M. Leduc, R. Pelton, Colloids Surf. A 317 (2008) 535–542.
[78] L. Dahne, S. Leporatti, E. Donath, H. Möhwald, J. Am. Chem. Soc. 123 (2001) 5431–5436.
[79] M.V. Voinova, M. Rodahl, M. Jonson, B. Kasemo, Phys. Scr. 59 (1999) 391–396.
[80] J. Choi, M.F. Rubner, Macromolecules 38 (2005) 116–124.
[81] M. Salomäki, I.A. Vinokurov, J. Kankare, Langmuir 21 (2005) 11232–11240.
[82] C. Picart, C. Gergely, Y. Arntz, J.-C. Voegel, P. Schaaf, F.J.G. Cuisinier, B. Senger, Biosens. Bioelectron. 20 (2004) 553–561.
[83] A.C. Toma, M. de Frutos, F. Livolant, E. Raspaud, Biomacromolecules 10 (2009) 2129–2134.
[84] S. Lindhoud, W. Norde, M.A. Cohen Stuart, J. Phys. Chem. B 113 (2009) 5431–5439.
[85] K. Glinel, A. Moussa, A.M. Jonas, A. Laschewsky, Langmuir 18 (2002) 1408–1412.